Published in final edited form as:
Wound Repair Regen. 2009 ; 17(3): 447–455. doi:10.1111/j.1524-475X.2009.00492.x.

Dynamic changes after murine digit amputation: The MRL mouse digit shows waves of tissue remodeling, growth, and apoptosis

Dimitri L. Gourevitch, MD, **Lise Clark, DVM, PhD**, **Khamilia Bedelbaeva, MD, PhD**, **John Leferovich, MS**, and **Ellen Heber-Katz, PhD**
The Wistar Institute, 3601 Spruce Street, Philadelphia, PA 19104

Abstract

Digit re-growth following amputation injury proximal to the first phalangeal joint is not a property of mammalian wound healing. However, the regenerative potential observed in the MRL mouse invites a re-examination of this rule. In this study, healing was assessed in three mouse strains after amputation midway through the second phalangeal bone. Three distinct outcomes were observed though evidence for re-growth was observed only in the MRL mouse. Here, a blastema-like structure was seen along with apparent chondrogenesis, consistent with a histological profile of a regenerative response to injury. Analysis of trichrome staining and basement membrane changes, proliferation and apoptosis indicated that these processes contributed to the formation of new digit tissue. On the other hand, SW and B6 digits did not show evidence of growth with little mesenchymal BrdU incorporation or phosphorylation of H3.

INTRODUCTION

Epimorphic regeneration in response to acute injury is accompanied by blastema formation. In urodeles, for example, amputation of a limb results in the formation of a mitotically active distal cell mass (1–4). Moreover in newt limb, the observed formation of a regenerative blastema shares some of its molecular pathways with developmental processes (5–7) In mammals, an epimorphic regenerative wound blastema response has been reported in association with antler re-growth and after a through-and-through hole punch is made in the ear pinnae of rabbits (8–9).

Re-growth of digit tips (distal to the terminal phalangeal joint) in mammals is widely reported but its relationship to classical blastema formation is unclear. That this is similar to amphibian epimorphic regeneration comes from one observation that both are inhibited by a skin flap over the wound (8, 10–11). On the other hand, re-growth of digit tips following amputation without blastema formation has been observed in rodents (12) and has been clinically reported in humans (10,13).

The degree of anatomical restoration of the digit tip following amputation may be age-related with reduced re-growth in adult mammals (14) compared to juvenile or fetal individuals (10,13, 15–17). However, digit tip regeneration has been observed in older individuals (up to at least 85 years of age) (18–19). In utero, amputated digit-tips regenerate if the amputation occurs through a region of undifferentiated cells in which msx l is expressed. Digit re-growth proximal to the terminal phalangial joint does not, in fact, lead to regeneration whether during development, in the neonate, or in mature animals (7).

*Address correspondence to: heber-katz@wistar.org; 3601 Spruce Street, Philadelphia, PA 19104; +1-215-898-3710.

The MRL mouse forms a circular blastema following a through-and-through ear hole punch wound (20) similar to the rabbit. This wound-closure response is a characteristic unique to the MRL and its ancestral strain, the LG mouse, compared with mouse strains studied thus far. An obvious and important site in which to study a wound-healing response is the full digit. A recent report shows that the MRL neonate displays enhanced digit-tip regeneration (16). In the current study, digit amputations proximal to the terminal phalangeal joint were examined for three adult strains of mice: MRL, C57BL/6 and Swiss Webster. Significant cellular responses after wounding were evident in all strains as determined by histological and immuno-histochemical analysis. This included apparent chondrogenesis and osteogenesis. In the MRL digits, differences in collagen accumulation and in remodeling as determined by basement membrane breakdown, BrdU incorporation, phosphorylation of histone H3, and the appearance of fibroblast-like cells characteristic of blastema formation were seen. This, however, was then offset by an apoptotic response and the disappearance of the blastema-like structure. Finally, a new proliferative response is again seen at 2 months though a new digit is never formed. Thus, it appears that the MRL is unique in its effort to grow a digit but that this effort is continually thwarted.

MATERIALS AND METHODS

Mice

Female mice, ages 3–4 months, were used in all experiments. The MRL/MpJ (MRL) mice were obtained from the Jackson Laboratories (Bar Harbor, ME), the C57BL/6 (B6) mice were obtained from Taconic Laboratories (Germantown, NY), and the Swiss Webster (SW) mice were obtained from Charles River. Animals were maintained under standard conditions at the Wistar Institute Animal Facility (Philadelphia, PA) and the protocols were in accordance with institutional regulations.

Surgical Procedures

Mice were anesthetized with Ketamine/Xylazine (90/9 mg/kg, i.p.). Both hind feet were scrubbed with chlorohexaderm and rinsed with 70% ethanol. Using a #10 scalpel, the fifth digit on both feet was amputated at the level of 50% of the second phalanx. Bleeding was controlled using digital pressure and sterile gauze. Animals were observed during anesthetic recovery to assure hemostasis. They were euthanized at various times post surgery (1–4 weeks and 2 months) using CO2 for the purpose of obtaining histological specimens of the healing digits.

BrdU Labeling of Dividing Cells

BrdU (0.1%) was administered ad libitum in the drinking water of animals that were subjected to digit injury. BrdU was administered immediately after injury and throughout the experiment as previously described (21). Fresh BrdU was prepared every three days throughout the labeling period.

Histological Techniques

Tissue was treated with Carnoy’s fixative for 24 hours, followed by decalcification with Morse’s decalcifying solution for 24–48 hours as previously described (22) and subjected to final processing using a Citadel 1000 Shandon Tissue Processor (Thermo-Fisher) and then paraffin embedding. Later, 5-micron-thick sections were cut. Samples were collected from at least three separate animals for each time point/strain. Hematoxylin and eosin staining was used to evaluate gross tissue architecture and Masson’s trichrome staining was used to evaluate collagen distribution (23).

Quantitation of collagen deposition by trichrome staining

In this case, we used ImagePro v4.0 for image analysis by selecting blues from multiple areas in the sections and creating a “trichrome” color block. The number of “trichrome” pixels was determined within the injury and growth area (See Figure 1 supplement). The area was expressed in square microns and the final data was expressed as trichrome per square micron. The mean of 2–6 samples were plotted and standard errors calculated. This technique was used as previously described (23).

Immunohistochemistry

To examine mitotic activity in the area of injury, antibodies for BrdU (Roche, Mannheim, Germany cat. # 11 585 860 001; mouse biotinylated mab; 1:14 dilution) and phospho-histone H3 (Upstate Cell Signaling Solutions, Lake Placid, NY, cat. # 06–570; rabbit; 1:100 dilution) were used. Tissue sections were incubated with primary antibody for 16 hours at +4°C followed by blocking with 5% bovine serum albumin for 1 hour. After washing and for direct visualization of BrdU, an ABC reagent (Vector, cat # PK-6100) and peroxidase substrate (DAB kit, Vector, cat. # SK-4100) were used as described previously (21,24). For visualization of phospho-H3 staining, rhodamine-labeled goat anti-rabbit antibody (Molecular Probes, Invitrogen; cat. # A11036; 1:500) was used for 1 hour RT.

To visualize the basement membrane, antibodies against collagen type IV (Southern Biotechnology Associates, Inc. cat. # 1340–01; goat; 1:100 dilution), laminin derived from basement membrane (Sigma, cat. # L9393; rabbit; 1:150 dilution), and laminin γ-2 (Santa Cruz Biotechnology, Inc. cat.# sc-7652; goat; 1:100 dilution) were used. Samples were exposed to primary antibody overnight at 4°C and then secondary biotinylated anti-goat (Sigma, cat. # B-3148; 1:1000 dilution) and anti-rabbit (Sigma, cat. # B-5283; 1:1000 dilution) antibodies were used respectively. Specific signal was detected by consequent application of ABC (Vector; cat. # DK-6100) and DAB (Vector; cat. # SK-4100) reagents. The specimens were dehydrated, cleared and mounted.

Quantitation of BrdU and phospho-H3-positive (pH3) cells was carried out using the same method of evaluation. Cells were counted on still images at 10× magnification in the combined area above the edge of amputated bone and 75–100 microns down from this edge (see Figure 1 supplement). Each sample was counted twice, each time point included 2–6 samples, and the mean and standard error was determined.

TUNEL Analysis

Paraffin-embedded digits were sectioned at 5 um. For detection of apoptotic cells, the DermaTACS™ *In Situ* Apoptosis Detection Kit (Trevigen, Inc) was used as described. The kit is based on DNA end-labeling using TdT and modified nucleotides. Detection of incorporated molecules is achieved using a chromogenic substrate with a horseradish peroxidase detection system and with biotinylated anti-BrdU antibody. The tissue is then counterstained.

RESULTS

All studies involved bilateral amputation of the P5 digit at the midpoint of the 2nd phalange. The micrographs are of longitudinal sections from 1–4 weeks and at 2 months. Figure 1A shows H&E staining of digits from the three different mouse strains (B6, MRL, and SW) week 1 after injury. The amputation site is shown on a normal digit (Fig 1Aa). Examination of the dermis after injury displayed differences between the three strains in terms of a) inflammation and cellular infiltrates, b) local cell responses and c) evidence of remodeling

through differences in collagen staining and basement membrane changes. Differences continued through weeks 1–4 (Fig 1B) and at 8 weeks (Fig 2).

At the end of week 1 after amputation, the B6 mouse exhibited a minimal inflammatory cellular response, MRL showed a small degree of inflammation which subsided by week 2, and SW showed a massive neutrophil infiltrate which lasted 3 weeks (Fig 1A, B). Osteoblast responses were unique to B6 and seen in the dermis both directly below the amputation site and on the diaphysis (side of the bone) for weeks 1 and 2 (Fig 1A, B). Also, a likely chondrogenic response was seen in the MRL at week 8 at the injury site (Fig 2). Finally, a dermal fibroblast-like spindle-shaped cellular response seemed to be exclusive to the MRL tissue after injury, though there may have been a similar response in SW but hidden by inflammatory cells (see Fig 1A, B). This fibroblast-like response was most dramatic at weeks 1–2 and at week 8 (Fig 2) at the MRL injury site.

Changes in Tissue Collagen, Basement Membrane Integrity, and Re-epithelialization

Analysis of trichrome staining as an indicator of local collagen deposition and remodeling during the first 4 weeks (Fig 1B) is shown in Figure 3. The amount of collagen rose and peaked in MRL tissue at 2 weeks after injury and then fell to background levels. The B6 and SW tissues showed little change during the whole healing period.

Another aspect of remodeling, the re-establishment of the basement membrane after injury and its potential breakdown during healing was examined (Fig 4, Fig 2 Supplement). After amputation, the basement between the epidermis and dermis is eliminated and then reformed. The integrity of the basement membrane in these studies was measured by the level of laminin, of the epithelial cell-specific laminin γ-2 chain of laminin 5 or laminin 332, and of collagen type IV expression, essential components of the basal lamina. Distinct differences between strains were seen.

At week 1 after injury, an intact basement membrane, as indicated by closed arrows in Fig 4 or Fig 2 supplement, was found in both B6 and MRL digits. In B6, the basement membrane remained intact through week 4. In SW, the basement membrane was not re-established until week 2 and remained intact through week 4. On the other hand, the MRL basement membrane was significantly reduced or not seen between weeks 2 and 4.

At the end of week 1, re-epithelialization was seen in the MRL in all samples, in the B6 in some of the samples, and not at all in the SW. By week 2, all B6 samples had re-epithelialized, and by week 3 this was true for all SW samples.

BrdU and Phospho-Histone H3 (pH3) Labeling in Injured and Healing Tissue

From the time of injury, BrdU was given in the drinking water to detect cumulative uptake (see Figs 1B, 2) and thus total proliferative capacity. At week 1 after injury, the MRL digit showed a large number of BrdU-positive cells (Fig 1B) and the majority of those cells resembled fibroblast-like cells (Fig 1A). The amount of BrdU incorporation increased over the first two weeks (Fig 1B), fell dramatically at week 3, and disappeared by week 4 (data not shown). A second wave of BrdU incorporation was evident at 8 weeks in the MRL digit (Fig 2). This was seen in the dermis, epidermis, and at the end of the bone where active proliferation was apparent.

SW digits also showed BrdU staining between weeks 1–2 after injury (Fig 1B), but it was difficult to identify the cell types due to a gross inflammatory response. The B6 digit showed a low level of BrdU staining during the first 4 weeks with an increase in incorporation at week 8 (Figs 1B, 2).

To further explore the mitotic activity at the injury site, we examined expression of the phosphorylated form of the histone protein H3 (phospho-histone H3 or pH3) which appears during late G2 and M and then disappears. This is not cumulative and shows cells that are actively dividing.

As seen in Figure 5 and Table 1, pH3 staining was found at different locations in the three different strains. In B6 digits, besides basal epidermal labeling, there was a low level of pH3 labeling in the dermis at 1 week. After week 1, pH3 was located exclusively in the basal epidermis except at week 4 when there were large numbers of positive cells that were present in the periosteum (Fig 5).

In MRL digits (Fig 5), there was dermal pH3 staining mainly at week 1, less at week 2, and essentially none at weeks 3 and 4. Labeling was again seen at week 8 mainly in the dermis. In SW digits, there was pH3 expression in the dermis at weeks 1 and 2, though much less than that seen in MRL, and found mainly in hair follicles and associated with epidermis and epidermal downgrowths (Fig 5).

Analysis of the number of BrdU-positive and pH3-positive cells in the dermis over time after injury is presented in Fig 6. Though BrdU staining is cumulative and pH3 staining is transient and related to cell cycle, the two curves are similar in that MRL is higher early, is then reduced to the level of the other two strains, and is then again elevated by week 8. Week 2 is an exception and may be attributed to BrdU accumulation and proliferation between weeks 1 and 2 that is missed by the pH3 analysis.

TUNEL Staining

The disappearance of BrdU-labeled cells by week 3 and the reappearance of accumulated BrdU labeling and pH3 labeling in the MRL dermis at week 8 led us to examine the possibility of an apoptotic response in this tissue. TUNEL analysis was carried out on MRL digits at wks 1–3 (Fig 7). A low number of TUNEL-positive cells could be found in the epidermis and hair follicles at week 1 and in the dermis near the cut bone at week 2. However, at week 3, a massive number of TUNEL-positive cells throughout the dermis could be seen.

DISCUSSION

Limb re-growth in the amphibian following amputation is accompanied by the formation of a blastema at the wound site followed by differentiation into various tissues (1–7). Limb regeneration in mammals has not been observed, however one strain of mouse, the MRL mouse, has displayed the unusual ability to generate a wound blastema after a through-and-through ear punch injury from which normal tissue architecture is restored (20). The obvious question was whether this mouse was capable of forming a blastema in response to a digit amputation injury.

In this study, we compared the response in three strains of mice, B6, MRL and SW, to an amputation injury through the second phalangial bone. It was evident that each strain displayed a unique tissue dynamic from among the various components inherent to the wound healing process. We observed a distinct pattern of reaction to the injury for each strain in terms of the inflammation, collagen synthesis, and bone and soft-tissue remodeling including basement membrane formation and breakdown. The most striking differences were found in remodeling, the proliferative response and the apoptotic response to injury.

Cell Division and Cell Death

Limb regeneration in amphibians in accompanied by two prominent features at the wound site, the apical cap and the regeneration blastema. The apical cap is a thickened epithelial layer covering the wound site, and the regeneration blastema comprises a large pool of undifferentiated, fibroblast-like cells which accumulates just beneath the apical cap (3). Both of these features involve a proliferative phase as shown by H3-thymidine labeling of DNA (25).

In the current study, we assessed proliferation using BrdU, a thymidine analogue which is incorporated into DNA during S phase. Since this was a two month study and it was not clear when, or if, cell division was taking place, we sought a cumulative picture of DNA synthesis. Thus, BrdU was administered throughout the experiment. The most striking contrast among the three strains arose in the proliferative response seen in MRL. We observed a very high level of BrdU incorporation in weeks 1 and 2 after injury and again at week 8.

The degree of reduction of BrdU labeling at week 3 in the MRL digit was quite surprising. Either the cells underwent migration away from the wound site or they died. We examined the possibility that an apoptotic response accounted for the absence of tissue BrdU accumulation. The results of TUNEL analysis revealed a minimum of apoptosis at week 1 which increased slightly at week 2 and but then showed a massive level of apoptosis at week 3. This supported the idea that BrdU accumulation was eliminated because cells were being eliminated through cell death.

To further examine the proliferative response, we employed a second marker of cell division. The histone protein H3 becomes phosphorylated in late G2 and in M, at a later time point than BrdU incorporation. Moreover, this cell-cycle marker is transient in its appearance in individual cells and represents a snapshot of cell division. Thus, pH3 expression provides an important complementary temporal view of cell proliferation. Together, the pH3 and BrdU results indicate that only the MRL mouse shows significant proliferation. Since BrdU is still accumulating at week 2 though there is little pH3 labeling at day 14, this is consistent with a proliferative response which peaks somewhere between week 1 and 2 but is gone by the 14^{th} day. The TUNEL results, on the other hand, show yet another aspect of the process which is occurring during the following week, clearly indicating a loss of cells in the MRL by week 3. This is also supported by the pH3 results.

We also witnessed a second ‘wave’ of proliferation – proliferative activation in the blastemal area at two months after a relatively proliferation-calm period at the end of the first month, which can be observed in Fig 2 and which was characteristic only for MRL. We interpret these results to say that the MRL mouse is capable of an unusual dermal proliferative response that appears to generate a blastema-like structure but does not develop into a full digit since the cells do not survive. Thus, the MRL begins to generate a blastema, the cells undergo apopotosis, and the MRL tries again.

The involvement of coordinated proliferation and apoptosis are the major components of limb growth and digit formation during development (26,27). This has been attributed to members of the fibroblast growth factor (FGF) family on the proliferative side (28) and to bone morphogenic factor (BMP) signaling which is, on the one hand, responsible for early epithelial growth and apical ectodermal ridge (AER) formation (29) and, on the other hand, involved in cell death at later timepoints during interdigit formation (30). Also, BMP2 and BMP4 signaling to undifferentiated mesenchymal cells induces apoptosis whereas signaling to more differentiated mesenchymal cells promotes chondrogenesis (31–32). Moreover, BMPs can also act in a dose-dependent manner: at high concentrations inducing cell death,

whereas low doses increase cell proliferation. In another example, BMPs induce osteoblast differentiation which is mediated mainly via the Smad-signaling pathway, whereas chondrogenic differentiation may be transmitted by both Smad-dependent and independent pathways (33). It may be that the interplay among these molecules (34) is directing the MRL digit response to injury and that inappropriate microenvironmental signals lead to the inability to grow. It may also be that there is an absence or a lack of coordinated expression of patterning molecules such as members of the shh and wnt signaling pathways and hox genes (5, 35–36).

Tissue Remodeling

Remodeling of tissue after injury has been well described (37). Re-epithelialization of dermal wounds has been shown to be different in studies examining MRL vs other strains. MRL ear punch wounds re-epithelialize faster than B6 ear wounds (20). On the other hand, re-epithelialization is delayed in the MRL following thermal injury when compared to BALB/c mice (38).

In previous studies of MRL mouse ear hole closure, thermal skin injuries, and cardiac cryoinjuries, greater collagen synthesis along with enhanced protease responses were seen (20, 21, 24, 38). A similar response was noted after digit amputation in the current study. Collagen levels as indicated by trichrome staining peaked in the MRL digit at two weeks compared to little change in the other two mouse strains. The drop in collagen after that could suggest an increasing proteolytic response, similar to what has been seen in the ear (24) and the heart (21). This response would be consistent with the basement membrane breakdown seen in the MRL starting at two weeks in this report.

Does the basement membrane have an effect on the proliferative response? Classic studies in the amphibian show that the regenerative response occurs in the absence of a basement membrane and that its re-establishment leads to a cessation of regenerative growth followed by scar formation (4,39). Also, in the MRL ear hole injury, basement membrane breakdown corresponds to the formation of the blastema and growth (24). In the digit, the basement membrane is disrupted upon injury and then re-establishes itself at one week in the MRL. Much of the proliferative response occurs during the first week as shown by BrdU incorporation and by pH3 staining and could be driven by events and molecules expressed before the membrane reforms.

One scenario to explain the next set of events would be that upon formation of the basement membrane, the cells would stop growing and start producing collagen, peaking at 2 weeks (Fig 3). Collagen production would then trigger a protease response which would lead to a reduction in collagen after 2 weeks and the disappearance of the basement membrane. Inappropriate signals would then lead to cell death instead of proliferation. However, the MRL digit subsequently re-initiates proliferation during the second 4 weeks. In the end, the component events that lead to a full regenerative response may be truncated or may not be properly coordinated in the MRL and thus the digit does not grow.

In conclusion, digit re-growth in adult B6 and SW mice is very similar to that seen in studies of limb regeneration in the rat with little evidence of tissue growth (40). On the other hand, the MRL mouse has some similarities to what is seen in the rat after limb amputation when adjacent muscle is still present. Here, limited cartilaginous and dermal blastema-like growth is seen. This is also seen in electrically-stimulated tissue (15) and in the very young rat (40). Collectively, the presence of a proliferating cell mass, basement membrane breakdown, collagen deposition, complete and early re-epithlialization, and an ongoing apoptotic response is suggestive of a regenerating blastema-like structure unique to the MRL mouse.

Supplementary Material

Refer to Web version on PubMed Central for supplementary material.

Acknowledgments

These studies were supported in part by grants from: the G. Harold and Leila Y. Mathers Charitable Foundation, W.W. Smith Foundation, the F.M. Kirby Foundation, and an NCI Cancer Center Grant (P30 CA10815) to the Wistar Institute. We would also like to thank Jon Mogford and DOD/DARPA for their long-term interest and support through Grant No W911NF-06-1-0067.

References

1. Smith AR, Lewis JH, Crawley A, Wolpert L. A quantitative study of blastemal growth and bone regression during limb regeneration in Triturus cristatus. J Embryol Exp Morphol. 1974; 32:375–90. [PubMed: 4463209]
2. Carlson BM. Some principles of regeneration in mammalian systems. Anat Rec B New Anat. 2005; 287:4–13. [PubMed: 16308859]
3. Brockes JP. Amphibian limb regeneration: rebuilding a complex structure. Science. 1997; 276:81–7. [PubMed: 9082990]
4. Stocum, DL. Regenerative Biology and Medicine. Burlington, MA: Academic Press/Elsevier; 2006. Regeneration of Appendages; p. 363-404.
5. Muneoka K, Bryant SV. Evidence that patterning mechanisms in developing and regenerating limbs are the same. Nature. 1982; 298:369–71. [PubMed: 7088182]
6. Nye HL, Cameron JA, Chernoff EA, Stocum DL. Regeneration of the urodele limb: a review. Dev Dyn. 2003; 226:280–94. [PubMed: 12557206]
7. Han M, Yang X, Taylor G, Burdsal CA, Anderson RA, Muneoka K. Limb regeneration in higher vertebrates: developing a roadmap. Anat Rec B New Anat. 2005; 287:14–24. [PubMed: 16308860]
8. Neufeld DA. Bone healing after amputation of mouse digits and newt limbs: implications for induced regeneration in mammals. Anat Rec. 1985; 211:156–65. [PubMed: 3977084]
9. Singer M, Weckesser EC, Geraudie J, Maier CE, Singer J. Open finger tip healing and replacement after distal amputation in rhesus monkey with comparison to limb regeneration in lower vertebrates. Anat Embryol (Berl). 1987; 177:29–36. [PubMed: 3439635]
10. Illingworth CM. Trapped fingers and amputated finger tips in children. J Pediatr Surg. 1974; 9:853–58. [PubMed: 4473530]
11. Mescher AL. Effects on adult newt limb regeneration of partial and complete skin flaps over the amputation surface. J Exp Zool. 1976; 195:117–28. [PubMed: 1255117]
12. Borgens RB. Mice regrow the tips of their foretoes. Science. 1982; 217:747–50. [PubMed: 7100922]
13. Vidal P, Dickson MG. Regeneration of the distal phalanx. A case report. J Hand Surg [Br]. 1993; 18:230–3.
14. Zhao W, Neufeld DA. Bone regrowth in young mice stimulated by nail organ. J Exp Zool. 1995; 271:155–9. [PubMed: 7884389]
15. Becker RO. Stimulation of partial limb regeneration in rats. Nature. 1972; 235:109–11. [PubMed: 4550399]
16. Chadwick RB, Bu L, Yu H, Hu Y, Wergedal JE, Mohan S, Baylink DJ. Digit tip regrowth and differential gene expression in MRL/Mpj, DBA/2, and C57BL/6 mice. Wound Repair Regen. 2007; 15:275–84. [PubMed: 17352761]
17. Masaki H, Ide H. Regeneration potency of mouse limbs. Dev Growth Differ. 2007; 49:89–98. [PubMed: 17335430]
18. Soderberg T, Nystrom A, Hallmans G, Hulten J. Treatment of fingertip amputations with bone exposure. A comparative study between surgical and conservative treatment methods. Scand J Plast Reconstr Surg. 1983; 17:147–52. [PubMed: 6361983]

19. Buckley SC, Scott S, Das K. Late review of the use of silver sulphadiazine dressings for the treatment of fingertip injuries. Injury. 2000; 31:301–4. [PubMed: 10775681]
20. Clark LD, Clark RK, Heber-Katz E. A new murine model for mammalian wound repair and regeneration. Clin Immunol Immunopathol. 1998; 88:35–45. [PubMed: 9683548]
21. Leferovich JM, Bedelbaeva K, Samulewicz S, Zhang XM, Zwas D, Lankford EB, Heber-Katz E. Heart regeneration in adult MRL mice. Proc Natl Acad Sci USA. 2001; 98:9830–5. [PubMed: 11493713]
22. Vinarsky V, Atkinson DL, Stevenson TJ, Keating MT, Odelberg SJ. Normal newt limb regeneration requires matrix metalloproteinase function. Dev Biol. 2005; 279:86–98. [PubMed: 15708560]
23. Broide DH, Lawrence T, Doherty T, Cho JY, Miller M, McElwain K, McElwain S, Karin M. Allergen-induced peribronchial fibrosis and mucus production mediated by IκB kinase β-dependent genes in airway epithelium. Proc Natl Acad Sci U S A. 2005; 102:17723–17728. [PubMed: 16317067]
24. Gourevitch D, Clark L, Chen P, Seitz A, Samulewicz SJ, Heber-Katz E. Matrix metalloproteinase activity correlates with blastema formation in the regenerating MRL mouse ear hole model. Dev Dyn. 2003; 226:377–87. [PubMed: 12557216]
25. Hay ED, Fischman DA. Origin of the blastema in regenerating limbs of the newt Triturus viridescens. An autoradiographic study using tritiated thymidine to follow cell proliferation and migration. Dev Biol. 1961; 3:26–59. [PubMed: 13712434]
26. Clarke PG. Developmental cell death: morphological diversity and multiple mechanisms. Anat Embryol (Berl). 1990; 181:195–213. [PubMed: 2186664]
27. Tickle C. Making digit patterns in the vertebrate limb. Nat Rev Mol Cell Biol. 2006; 7:45–53. [PubMed: 16493412]
28. Miyake A, Konishi M, Martin FH, Hernday NA, Ozaki K, Yamamoto S, Mikami T, Arakawa T, Itoh N. Structure and expression of a novel member, FGF-16, on the fibroblast growth factor family. Biochem Biophys Res Commun. 1998; 243:148–52. [PubMed: 9473496]
29. Pizette S, Abate-Shen C, Niswander L. BMP controls proximodistal outgrowth, via induction of the apical ectodermal ridge, and dorsoventral patterning in the vertebrate limb. Development. 2001; 128:4463–74. [PubMed: 11714672]
30. Zuzarte-Luis V, Hurle JM. Programmed cell death in the embryonic vertebrate limb. Semin Cell Dev Biol. 2005; 16:261–9. [PubMed: 15797836]
31. Boulet AM, Moon AM, Arenkiel BR, Capecchi MR. The roles of Fgf4 and Fgf8 in limb bud initiation and outgrowth. Dev Biol. 2004; 273:361–72. [PubMed: 15328019]
32. Guha U, Gomes WA, Kobayashi T, Pestell RG, Kessler JA. In vivo evidence that BMP signaling is necessary for apoptosis in the mouse limb. Dev Biol. 2002; 249:108–20. [PubMed: 12217322]
33. Fujii M, Takeda K, Imamura T, Aoki H, Sampath TK, Enomoto S, Kawabata M, Kato M, Ichijo H, Miyazono K. Roles of bone morphogenetic protein type I receptors and Smad proteins in osteoblast and chondroblast differentiation. Mol Biol Cell. 1999; 10:3801–13. [PubMed: 10564272]
34. Pajni-Underwood S, Wilson CP, Elder C, Mishina Y, Lewandoski M. BMP signals control limb bud interdigital programmed cell death by regulating FGF signaling. Development. 2007; 134:2359–68. [PubMed: 17537800]
35. Schnapp E, Kragl M, Rubin L, Tanaka EM. Hedgehog signaling controls dorsoventral patterning, blastema cell proliferation and cartilage induction during axolotl tail regeneration. Development. 2005; 132:3243–53. [PubMed: 15983402]
36. Yokoyama H, Ogino H, Stoick-Cooper CL, Grainger RM, Moon RT. Wnt/beta-catenin signaling has an essential role in the initiation of limb regeneration. Dev Biol. 2007; 306:170–8. [PubMed: 17442299]
37. Clark, R. The Molecular and Cellular Biology of Wound Repair. New York, NY: Plenum Press; 1996. Wound repair: Overview and General Consideration; p. 3-35.
38. Davis TA, Amare M, Naik S, Kovalchuk AL, Tadaki D. Differential cutaneous wound healing in thermally injured MRL/MPJ mice. Wound Repair Regen. 2007; 15:577–88. [PubMed: 17650103]

39. Stocum DL, Crawford K. Use of retinoids to analyze the cellular basis of positional memory in regenerating amphibian limbs. Biochem Cell Biol. 1987; 65:750–61. [PubMed: 3325080]

40. Libbin RM, Weinstein M. Sequence of development of innately regenerated growth-plate cartilage in the hindlimb of the neonatal rat. Am J Anat. 1987; 180:255–65. [PubMed: 3434542]

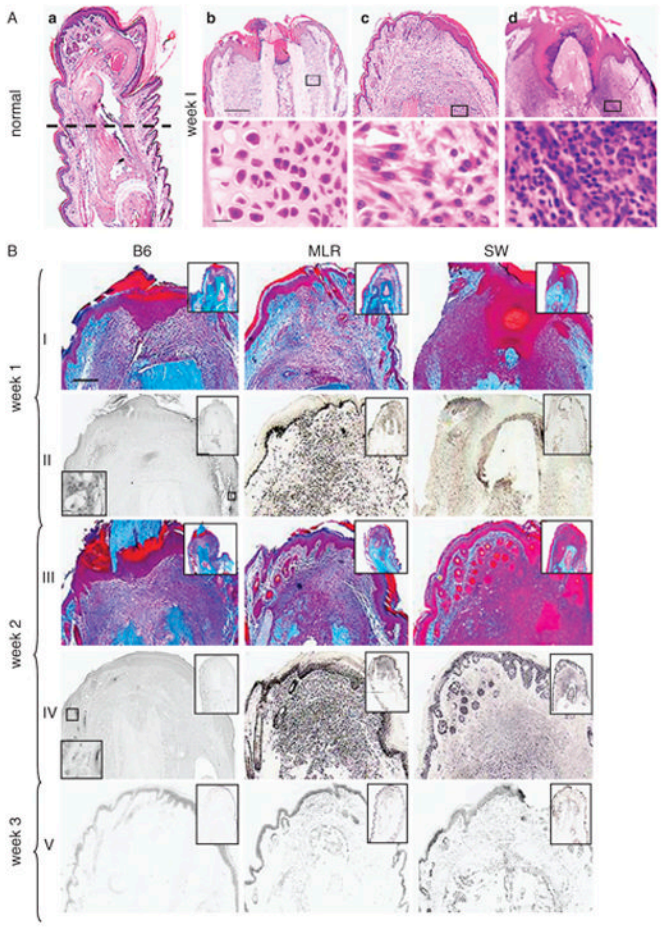

Figure 1. Digit tissue sections post-injury over a 4 week period

Fig 1A. On the left hand side is a longitudinal H&E section of an uninjured MRL digit (1Aa).

The broken line indicates the level at which each digit was subjected to amputational injury. In the panels to the right are amputated digits week 1 post-injury **(upper row scale bar = 300 microns; lower row scale bar = 15 microns)** from C57BL/6 (1Ab), MRL/MpJ (1Ac), and Swiss-Webster mice (1Ad). The lower panels come from the area adjacent to the bone as indicated by rectangles.

Fig 1B. Trichrome-stained and BrdU-labeled digit tissue sections weeks 1–3 post-injury. Longitudinal sections of digits are shown at various times after injury. Each strain of mouse is indicated by the column label. Row labels indicate the time after injury. Digit sections from week 1 (row I) and week 2 (row III) were stained with Masson's trichrome stain. Alternate rows show BrdU staining for week 1 (row II), week 2 (row IV), and week 3 (row V). **The lower left inset shows that BrdU did stain in the basal epidermis. The scale bar shown in row I (applies to all rows) = 200 microns; the scale bar in the upper inset = 600 microns and in the lower inset = 15 microns.**

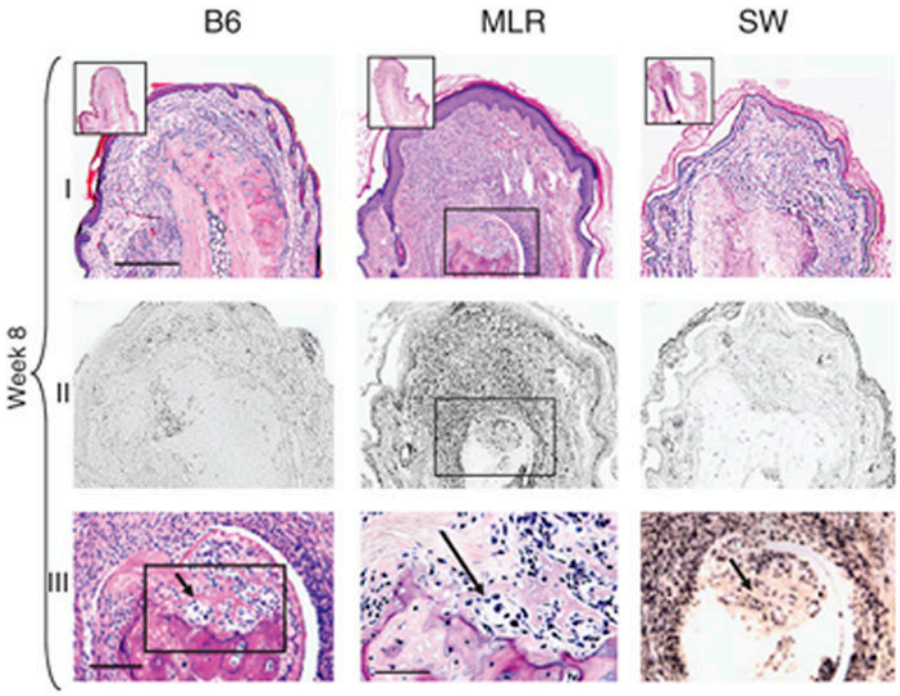

Figure 2. H&E and BrdU-stained digit tissue sections eight weeks post-injury

Longitudinal sections of digits from B6, MRL, and SW mice 60 days after injury are shown either stained with H& E (row I) or with anti-BrdU antibody (row II). In row III, from left to right, is an increasingly higher magnification of the region showing chondrogenesis in the MRL digit. The figure on the left is derived from the boxed region of the MRL from row I showing H&E staining. The middle figure is derived from the boxed region from the figure to its left. The arrows indicate groups of chondrocytes on the tip of the remodeled bone stump. **In the right-hand panel, row III, the same area showing BrdU incorporation in chondrocytes can be seen. The scale bar in row I (applies to rows I & II) = 300 microns; the scale bar in the upper inset, row I = 400 microns; in row III, left and right panels = 200 microns and in middle panel = 150 microns.**

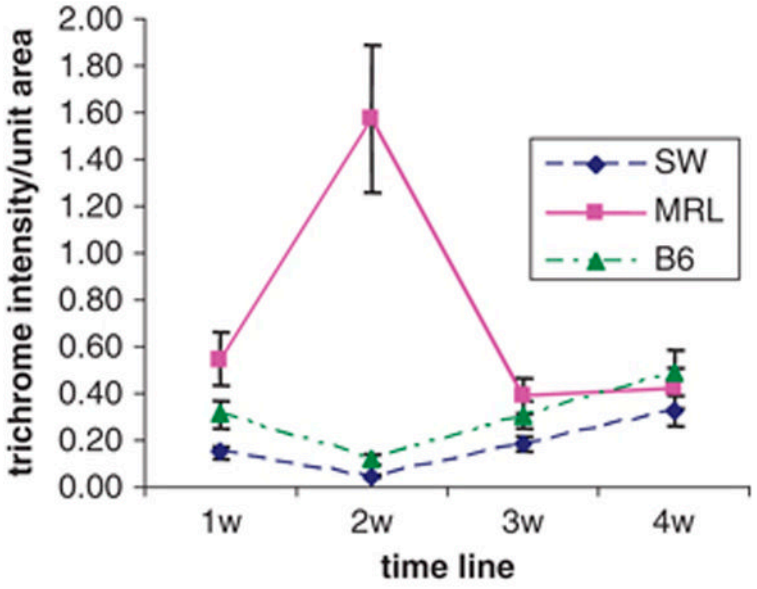

Figure 3. Quantitation of trichrome staining

Masson trichrome staining of injured digits as shown in Fig 1B was analyzed by Image-Pro4. The plot analyzes trichrome-positive deposition in the blastema area (wound site around and above the bone as indicated in Fig. 1 Supplement). The mean and standard errors of 2–6 samples per time point are shown.

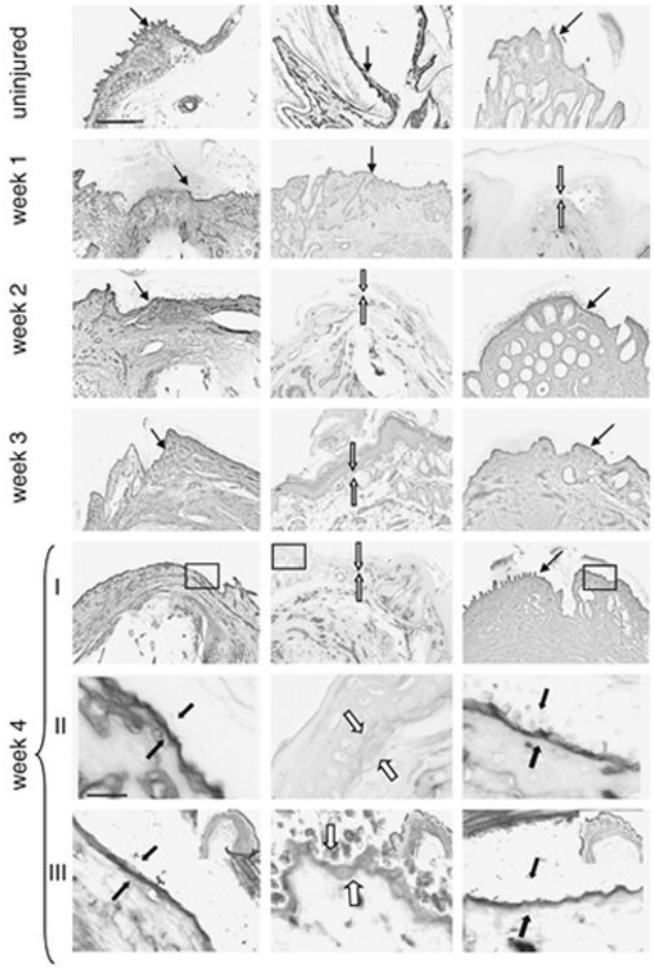

Figure 4. Immunohistochemical staining of basement membrane

Uninjured and injured (amputated) digits from weeks 1, 2, 3, and 4 (rows I–II) post injury were stained with antibody to collagen type IV, visualized using DAB precipitation. The arrows indicate the location of the basement membrane between the dermis and epidermis, with closed arrows for the presence of and open arrows for the absence of basement membrane. At week 4 (row II), photomicrographs at a higher magnification of the boxed regions in row I can be seen. At week 4 (row III), sections stained with anti-laminin gamma-2 antibody are shown and are derived from the boxed regions presented in the upper right insets. **The scale bar seen in the top row, first panel (applies to top 5 rows) = 150 microns; the scale bar seen in week 4, row II (applies to lower two rows) = 20 microns.**

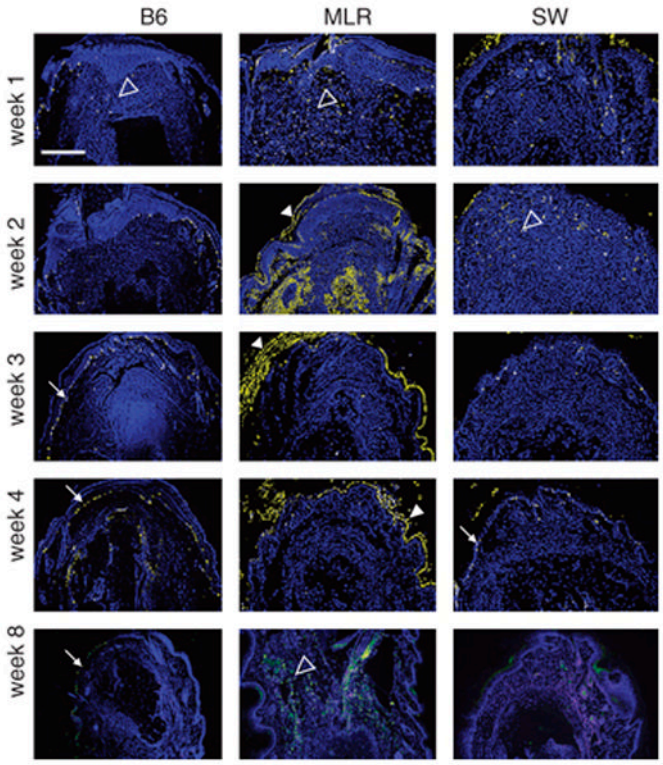

Figure 5. Phospho-histone H3 (pH3) immunohistochemistry

Longitudinal sections of digits stained for pH3 at various times after injury. Column labels indicates the strain. Row labels correspond to the time after injury. The photomicrographs were converted from red fluorescent staining to yellow with a blue DAPI counter stain for nuclei. The scale bar **seen in the upper left panel (applies to all panels) = 350 microns.** Staining in the basal epidermis (closed white arrows), in the dermis (open white arrowheads), and in the superficial keratin layer (closed white arrowheads) are shown and as presented in Table 1.

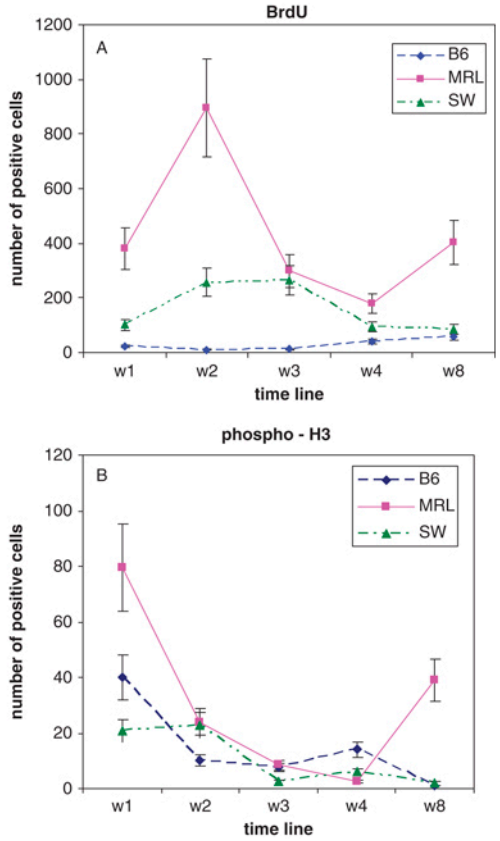

Figure 6. Quantitation of BrdU and pH3-positive cells in the dermis of injured digits

The plots analyze proliferative cells found in the dermis from week 1 to week 8. In Figure 6A, BrdU-positive cells are represented and in Fig 6B, pH3-positive cells are represented. The X-axis shows the time points and the Y-axis shows the number of cells in the wound site around and above the bone. The mean and standard errors of 2–6 samples per time point are shown.

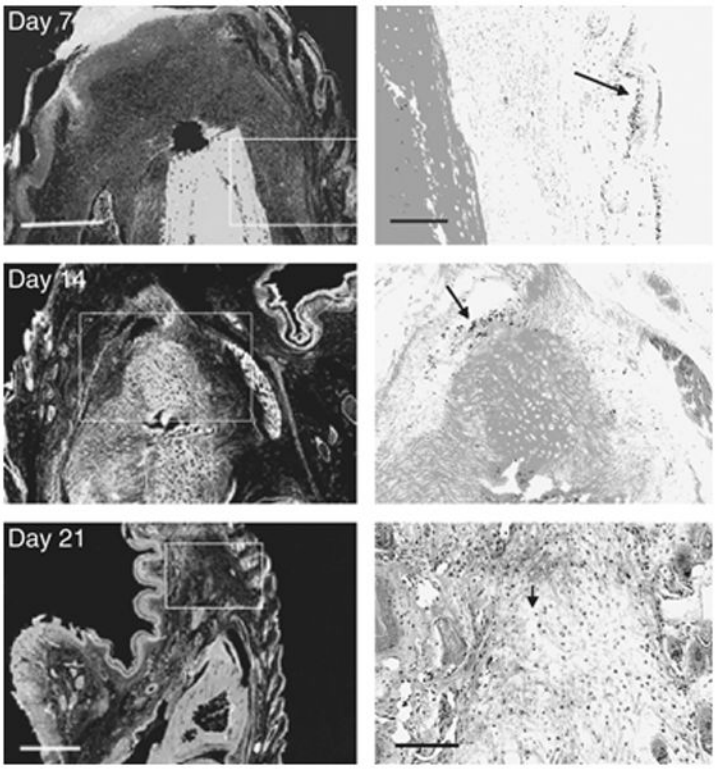

Figure 7. TUNEL staining of MRL digits

Longitudinal sections of injured MRL digits stained for TUNEL-positive cells at various times after injury. At week 1 post-injury (upper panels), TUNEL staining was rare and shown here in the basal epidermis (arrow). At week 2 post-injury (middle panels), there were limited TUNEL-positive cells (arrows) in the dermis found distal to the bone. At week 3 post-injury (bottom panels), TUNEL-positive cells were found throughout the dermis. **The scale bars for the left panels (Day 7 and 14) = 150 microns and the right panels (Day 7 and 14) = 50 microns; the scale bar for the left panel (Day 21) = 600 microns and for the right panel (Day 21) = 150 microns.**

TABLE 1

Phosphorylated histone H3 expression in digits

Week	B6	MRL	SW
1	dermis *	dermis	basal epidermis
	epidermis	epidermis	dermis
		basal epidermis	epidermis
			hair follicle
2	basal epidermis	basal epidermis	epidermis
	dermis (rare)	dermis	dermis
		epidermis	hair follicle
		superficial keratin layer	
3	basal epidermis	superficial keratin layer	epidermis
	dermis (rare)	dermis (rare)	
4			**basement**
	basal epidermis	superficial keratin layer	membrane
	periosteal area	epidermis	epidermis
8	basal epidermis	dermis	superficial keratin layer
			single cells in dermis

* Listed in order of intensity of staining